A Multi Agent Simulation Model for Estimating Knock-on Train Delays under High-Frequency Urban Rail Operation

Seiji IWAKURA [a], Kotaro KAWAMURA [b], Ryuta TSUNODA [c],
Ikuto TAKAHASHI [d]

[a] *Department of Civil Engineering, Shibaura Institute of Technology, 1-7-5 Toyosu, Koto-ku, Tokyo,135-8548, Japan; E-mail: iwakura@shibaura-it.ac.jp*
[b,c] *Graduate School of Engineering and Science, Shibaura Institute of Technology, 1-7-5 Toyosu, Koto-ku, Tokyo,135-8548, Japan*
[b] *E-mail: me13024@shibaura-it.ac.jp*
[c] *E-mail: me13055@shibaura-it.ac.jp*
[d] *Road Management Division, Chigasaki city,1-1-1Chigasaki, Kanagawa, 253-8686, Japan*

Abstract: The decreasing travel time reliability of urban railway services in the Tokyo Metropolitan Area is the result of the train delays in daily morning hour period. The proposed multi agent simulation model is developed to analyze train knock-on delay in a 48.3 km track length from Nagatsuda station of the Denentoshi line to Oshiage station of the Hanzomon line. The simulation part consists of a train traffic simulator and a passenger flow simulator with that works in parallel. The errors in the delay estimation of individual trains by the proposed simulator are within the allowable limits in comparison to the actual train delay. Some forecasting results of investment strategies designed to reduce delay can be assessed.

Keywords: Knock-on train delay, Multi agent simulation, urban rail, High frequency operation

1. INTRODUCTION

To reduce the congestion of urban railways in the Tokyo metropolitan area, there has been a push to increase transportation capacity through the construction of multiple tracks and the provision of new lines. These measures require long-term development, so they are also accompanied by measures that include increasing the number of trains in operation, with improvements to the signaling system and measures to alleviate congestion at terminal stations by mutual direct operations. However, because of the bottlenecks caused by increases in the stopping time, high volumes of boarding/disembarking passengers, and differences in line capacity limits between different lines on the same track, train congestion occurs, resulting in delays spreading onto expanded mutual direct operation lines.

The goal of this study is to construct a simulation model that is able to quantitatively analyze the effects of anti-delay measures using urban lines that are operated at high frequency on the same track as our target. Delay refers to the difference between the arrival time listed on the time schedule and the actual arrival time.

For the purposes of this study, we have designated a 48.3 km section of tracks running from the Chuo-Rinkan Station on the Tokyu Denentoshi Line to the Oshiage Station on the Tokyo Metro Hanzomon Line as our target. Ten-car trains are operated in 2 minute intervals on this line. At peak hours, the congestion rate exceeds 180% from Ikejiri to Shibuya.

Following this, in Section 2, the conditions of delay and factors contributing to delays for the lines in question are considered. In Section 3, we explain the construction of the simulation sub models, the data used, and the reproducibility of these data. In Section 4, we summarize the results of this research.

2. CONDITIONS AND FACTORS THAT CAUSE TRAIN DELAYS

To analyze the actual conditions of delay from Nagatsuta Station on the Denentoshi Line to Hanzomon Station on the Hanzomon Line, we have used operator time tables for departures and operation record data, both in units of seconds, in which the arrival times, stopping times, and departure times for each station from 6–11 a.m. over 24 weekdays from November 15th to December 17th, 2010 were obtained from the automatic train control device.

The operation patterns for the target lines are shown in Figure 1. The trains, which have different end points and come in multiple varieties, are mixed together in operation.

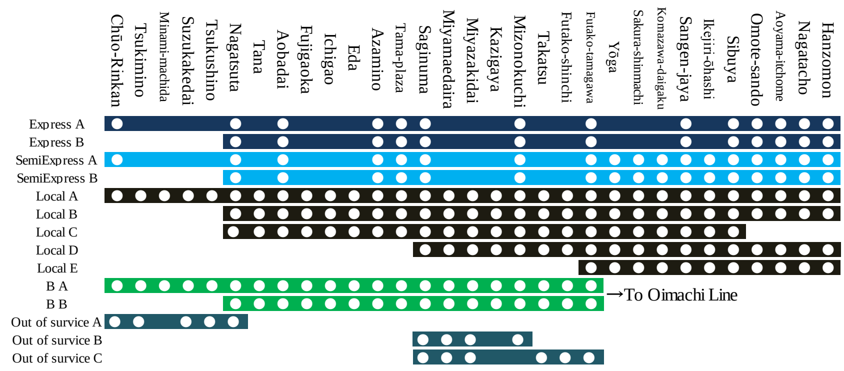

The number of trains (Arrived at Futako-tamagawa)
※November,15,2010, Morning Peak Time(5 to 11)

Type / Time	5-6	6-7	7-8	8-9	9-10	10-11
Express A	0	0	5	10	0	0
Express B	0	1	0	0	0	0
SemiExpress A	0	0	2	1	1	0
SemiExpress B	0	3	3	2	4	4
Local A	1	5	7	12	11	7
Local B	2	4	6	2	1	1
Local C	1	0	0	0	0	0
Local D	2	3	2	0	0	0
Local E	1	0	0	0	0	0
B B	0	0	0	0	0	1
B B	2	1	0	0	0	0

Figure 1. Train operation patterns for the Denentoshi line and Hanzomon line

Figure 2 shows the average value and standard deviation (±1σ) of the delay time for trains arriving at Hanzomon Station. Delays are assumed to start from the train arriving at Hanzomon around 7:30 and increase up until around 9:30, after which time they appear to settle. In terms of average values, the longest delay, slightly more than 8 minutes, occurs around 9:30.

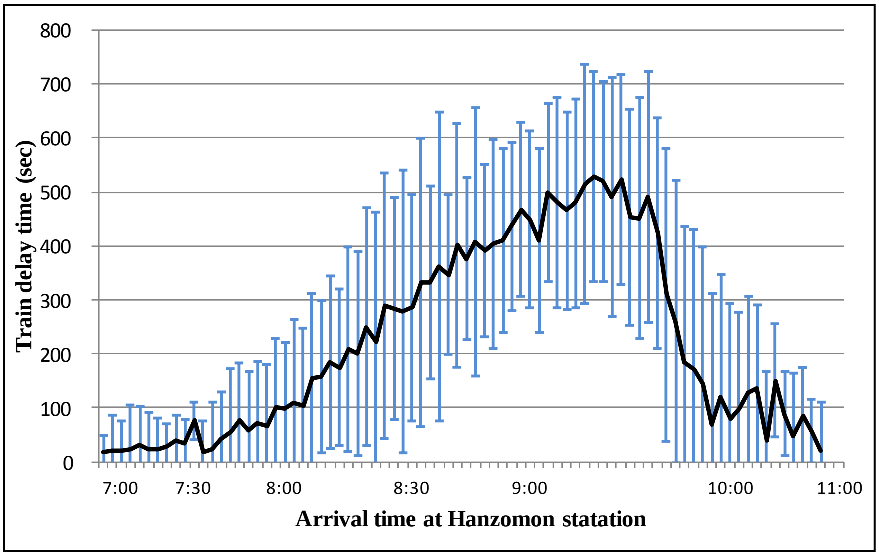

Figure 2. Average value and standard deviation of the delay time for trains arriving at Hanzomon Station

Next, using data for November 15, which show typical conditions that produce delay as an example, we classify the factors that cause delay as stopping delays and inter-station running delays. Figure 3 shows the "stopping delay," which is the sum of the differences between the stopping times listed on the time schedule and the actual stopping times at each station from Nagatsuta Station to Hanzomon Station, the "running delay," which is the sum of the differences between the inter-station running times listed on the time schedule (difference between station arrival and departure times) and the actual inter-station running time from Nagatsuta Station to Hanzomon Station, and the "total delay," which is the sum of the "stopping delay" and "running delay." Stopping delays occur across all times, but it is assumed that the total delay is kept under control through recovery operations, which negate the value of the running delay until about 8:00. However, because of further increases in stopping delays, delays cannot be fully absorbed by recovery operation, so there are sharp increases in the total delay. As the delays materialize, train congestion on the lines begins, making recovery operation difficult and the inter-station running time near 9:00 a.m. does not match what was set in the time schedule, thus triggering increases to the total delay. After this, with decline in demand and flexibility of the operation intervals approaching 10:00 a.m., recovery operation is undertaken to reduce the total delay.

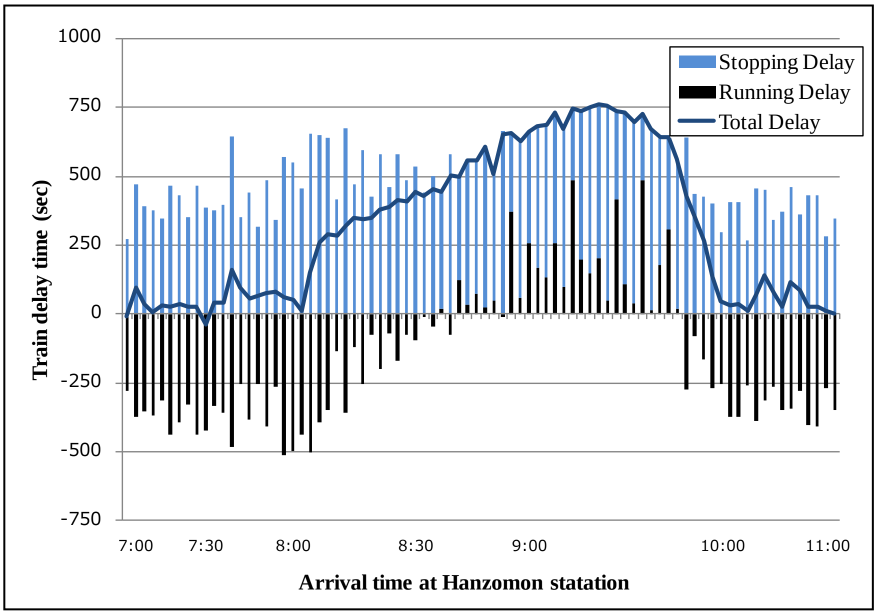

Figure 3. Stopping delays, running delays and total delays for trains arriving at Hanzomon Station

The delays can be controlled as long as recovery operation is used to compensate for stopping delays, but as seen in Figure 3, it is recognized that even on other days there is a tendency for recovery operation to become difficult where stopping delays occur in succession for a total of 600 or more seconds after 8:00 a.m.

To confirm the conditions for knock-on train delays, data for three days with varying degrees of delay were averaged and these data are shown in Figure 4. At 7:30 a.m. delays occur from Hanzomon, along with knock-on delays at Aoyama-itchōme Station, and expand to the trains that follow on the Denentoshi Line until around 8:30 a.m. After this, a reduction in delays can be seen from Sangenjaya Station. However, delays on the Denentoshi Line have now spread to the Hanzomon Line and have expanded even further onto the Hanzomon n section of tracks.

From the above, routine delays can be observed on the Denentoshi Line as well as the Hanzomon Line, and an average arrival delay of 500 seconds occurs just after 9:00 at Hanzomon Station. The initial delay occurs on the Hanzomon Line and through increases in the stopping time accompanied with a high congestion rate and large passenger volumes, the delays expand to a level where they cannot be compensated for by recovery operation. This spreads delays that have occurred on the inner-city section tracks to the trains that follow, and as the delays to the trains that follow remain unabsorbed, delays in the inner city continue to expand.

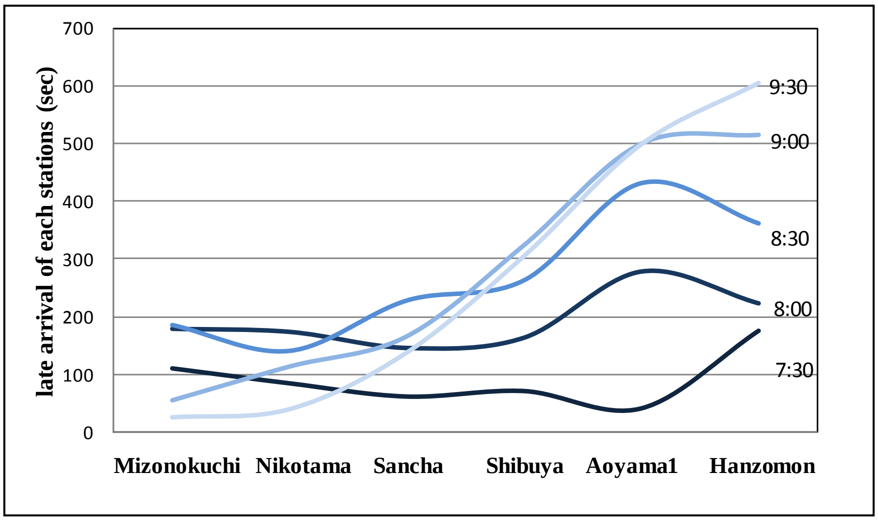

Figure 4. Conditions for knock-on train delays for each stations

3. THE SIMULATION MODEL

3.1 Overview of the Simulation Model

To accommodate the aims of this research, it is necessary to express the interaction between trains when they are near each other on a line, and the interaction between boarding and disembarking passengers when the train stops at a station. In order to express stopping time, which is particularly reliant on the boarding and disembarking behavior of users, it is necessary to incorporate a mechanism in which the users act autonomously. For the purposes of producing a simulation that includes the running time and stopping time, the high affinity of a multi-agent simulation was considered.

The programming software that was used to create the model is artisoc academic 3.0 from KOZO KEIKAKU ENGINEERING Inc.

Following the definition of time, the model integrates a sub-model that estimates the inter-station r unning time, a sub-model that estimates the boarding and disembarking time, as well as a sub-model that estimates the confirmed time and adjusted time, forming a structure that expresses the running of all trains on the target section of tracks in the peak time range as well as the boarding and disembarking behavior at all stations.

Furthermore, the inter-station running time is the time required for a train to depart from a station and arrive at the next station. The boarding and disembarking time is the time required for passengers to board and to disembark from the train. In addition, the adjusted time is the time from the point when passengers have completed boarding/disembarking to the point when the doors close and the confirmed time indicates the difference from the point when the train doors have closed to the time when the train has begun to move.

Below, we explain the construction, the data used, and the reproducibility of each sub-model as well as of the integrated model.

3.2 The Inter-station Running Time Estimation Model

3.2.1 Model Rule Settings

The model follows the actual ATC signal codes for given conditions with a pitch of 0.2 seconds and operates using the following rules, in an almost identical principle to actual operating methods.

Rule 1: If the departure time on the time schedule passes and a preceding train does not exist ahead in the block section, the train is powered with acceleration at startup of 3.3 km/h/s.

Rule 2: The end positions of preceding trains in the 16 block sections ahead are detected to run trains at the allowable section speed, in response to the signal code from the position of trains ahead. Moreover, depending on the positional relationship with the preceding trains, and following the pattern of the signal deployment plan, the allowable section speed is fixed at 15 levels max. for the Denentoshi Line and 9 levels max. for the Hanzomon Line.

Rule 3: If a preceding train does not exist until one of the 16 block sections ahead, operation is allowed to proceed at a section speed of −10 km/h.

Rule 4: When decelerating, the train is run at with a = −3.5 km/h/s and x as the distance to the stopping line.

Rule 5: The acceleration/deceleration is influenced by the inclination of the line: $a((km/h)/s) = 3.3 - 0.035i(‰)$ $a((km/h)/s) = 3.3 - 0.035i(‰)$. For example, with a 20% incline, acceleration/deceleration changes by approximately 23%.

Rule 6: If a station with a stopped train is near, the train will stop at the train stopping position in accordance with the speed stated in Rule 4.

3.2.2 Data Used to Construct the Model

(1) Signal code table: From the ATC signal codes, system data such as block sections, speed signals, inclines, wiring, and station positions are reflected on the lines in the system space.

(2) Station platform drawings: Used to designate where trains will stop at each station.

(3) Train performance table: The 5000 Series, which is a typical train on the Denentoshi Line, has a combined car length of 200 m, max. speed of 110 km/h, acceleration speed of 3.3 km/h/s, and a deceleration speed of 3.5 km/h/s.

(4) Time table of arrivals and departures: The departure time and stopping time in 10-second units, as they appeared on the time schedule, were used. Moreover, in the integrated model described below, because the stopping time is estimated from the model, it does not need to be produced externally.

In addition to the above, the following was used to confirm and improve reproducibility:

(5) Operation record data: In order to understand the actual conditions of delay, the arrival times, stop times, and departure times for each station in seconds were collected. These data were obtained from the automatic train control device over a period of 24 weekdays from November 15th to December 17th, 2010 from 6 to 11 am. The automatic train control device applies corrections and calculates the short circuit time for entering and leaving a track circuit that is occupied when a train is stopped at a station, and the actual departure and arrival time has an error margin of about 10 seconds.

3.2.3 Accuracy of the Model

Below, we externally produce the actual stop times to explain the reproducibility of simulation results from Nagatsuta Station to Hanzomon Station over a period of 24 weekdays. The results of calculating the residual RMS between the estimated value and actual value for the arrival time, for all trains for 12 stations where the express train stops from Aobadai Station to Hanzomon station, show an average of about 10.3 seconds. Figure 5 shows the residual average value and standard deviation for the arrival time, as well as the residual maximum and minimum value. It was understood that it could be kept to within 20 seconds even with a residual average of +1 standard deviation for th be obtained for the coefficient of correlation between the estimated value and actual value for the required time, which is the sum total of the estimated value for the interstation running time from Nagatsuta Station to Hanzomon Station and the actual value of the station stopping time.

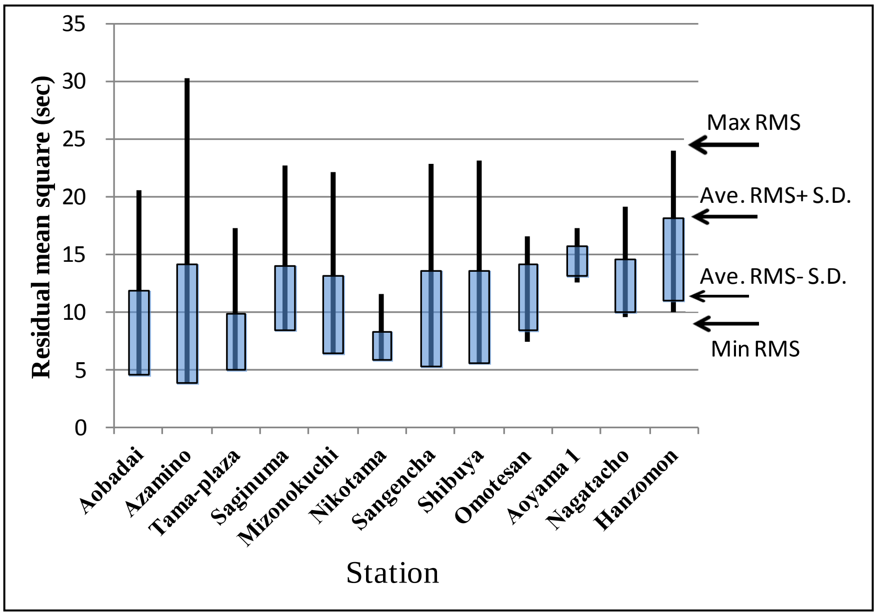

Figure 5. Residual average value and standard deviation for the arrival time for each stations

Below, we describe the coefficient of correlation between the residual for the estimated value of the arrival time organized by train type, the estimated value for the required time (as mentioned above, the sum value of the estimated value for the inter-station running time and the actual value of the station stopping time), and the actual value.

The average residual for the arrival time of express trains at 12 stopping stations from Aobadai Station to Hanzomon Station is 11.4 seconds and the coefficient of correlation for the required time is at least 0.98.

The average residual for the arrival time of semi-express trains is 10 seconds and the coefficient of correlation for the required time ranges from 0.87 to 0.97 depending on the day. The residual for the arrival time at each station for the semi-express train is about 15 seconds, with the exception of Ikejiri-Ōhashi.

3.3 Boarding/Disembarking Estimation Model

3.3.1 Model Rule

Stopping time is generally determined by the doors with the largest volume of people boarding onto, and disembarking from, a crowded train car. When creating this model, we specified a door that takes the most time for boarding and disembarking to acquire boarding/disembarking behavior and setup the rules. The model operates with a 0.2 second pitch.

The system space is one-quarter of a train car that has a door at its center. The diameter of an individual boarding and disembarking passenger is set to 40 cm, and passenger agents are categorized into three groups of passengers: disembarking, reboarding, and boarding. These attributes are then sorted into gender and incidental behaviors (e.g., in which the passenger looks at their cellular phone while boarding the train). In addition, the number of passengers riding each train at each station is set from actual values obtained from video observation and the metropolitan traffic census. Also, the set measurement for the walking speed from Rule 2 to Rule 5 is based on the measured value for the boarding speed, which was measured from video images using the 2D video measurement software Move-tr/2D after providing positional coordinates. Furthermore, as a result of using an acceleration to acquire the proper boarding speed data four times as video was being captured to analyze the accuracy of boarding speeds from the positional coordinates, it was confirmed that there is a margin of error of about so, .

Using this method, the actual boarding and disembarking behavior was analyzed to set up the following rules.

Rule 1: When the train arrives at the station, passenger agents disembarking at the corresponding station, and continuing passengers who are standing near the door, will exit to the platform, and re-boarding passengers will then perform the action of coming back into the train. Disembarking passenger agents will head from inside the train to the platform and the number of other boarding and disembarking passengers 20 cm ahead are counted in 180 degrees ahead that are equally spaced in 45 degree sections in five directions to avoid and move in the direction with the least amount of agents.

Rule 2: For the initial value for the walking speed, a uniform random number is used to increase the speed from 0 to 5 to 30 cm/s every 0.2 seconds while boarding, and the upper limit for the speed is 130 cm/s. For the walking speed settings organized by passenger attributes, from the results of actually measuring video images, the male–female ratio was set to 7:3 and the initial speed was set as 1x for males and 0.9x for females. The number of passengers that perform incidental behaviors, such as using a cellular phone, from the results of actual measurements, was set to 5% of the number of boarding passengers and, in terms of walking speed, they moved at 0.68x the speed of passengers ahead.

Rule 3: Those passengers who become reboarding passenger agents are continuing passengers who stand in a 160 cm × 160 cm space that connects to the door for disembarkation, become an obstacle for disembarkation, and then temporarily disembark onto the platform. After temporarily disembarking, they remain on the platform near the door.

Rule 4: After processing for the disembarking passengers is complete, the boarding passengers and reboarding passengers come inside the train from the platform. For the boarding passenger and reboarding passenger agents, just as in Rule 1, the number of other disembarking and reboarding passengers 20 cm ahead is counted in 180 degrees ahead that are equally spaced in 45 degree sections in five directions to avoid and move in the direction with the least number of agents.

Rule 5: For the initial value of the boarding speed, a uniform random number is used to increase the speed from 0 to 5 to 30 cm/s every 0.2 seconds while the passengers are waiting in line to board and the upper limit for the speed is 130 cm/s. In addition, because of congestion inside the train, the speed is adjusted as personal space is secured.

Rule 6: The initial value for personal space is a 40 cm circle with each passenger agent at the center, and if another agent exists within a 40 to 20 cm radius of the passenger agent every 0.2 seconds, then the radius of the personal space for each agent will shrink by 1.6 cm every 0.2 seconds.

Rule 7: Boarding passenger agents accelerate at a walking speed of 8cm/s every 0.2s towards

space where other passengers do not exist in a each agent, if other passengers exist 80 cm ahead in the advancing direction, they enter the train while repeatedly decelerating so that their speed reduces to 8 cm/s every 0.2 seconds.
Rule 8: Agents will search for a position where there are no other passenger agents within an 80 cm radius, and the order of preference for standing positions following boarding onto the train is as follows: first, near the door that they boarded through; second, the left and right depths of the car; and third, near the door directly opposite the boarding door. As a result, the arrangement of passenger agents inside the train after boarding is adjusted so that areas near the door are avoided as much as possible and a consistent distance is maintained between passenger agents.
Rule 9: If passenger agents are pushed onto other passengers, they will decelerate at a walking speed of 4 cm/s every 0.2 seconds, and if passenger agents are not pushed, their straight walking speed will accelerate by 8 cm/s every 0.2 seconds, and if avoiding the left and right they will accelerate and advance at 4 cm/s. The pushing behavior occurs when 13 or more passengers exist in a 1.6 square meter range at the center of one-quarter of a train (equivalent to a congestion rate of 180%).

3.3.2 Data Used for the Model Structure

(1) Boarding/disembarking speed: Move-tr/2D ver. 7.0 was used to create per-second coordinates for individual passengers who were video-taped from the upper platform for the semi-express train at the most congested door from November 16 until December 10, 2010 on weekdays from 7:00–10:00, and the door passage speed for 294 trains was calculated. Passenger attributes (gender and incidental behaviors) were given. The disembarkation speed follows the same rules as boarding behavior, and therefore, it was not measured.
(2) Number of boarding and disembarking passengers: The number of boarding and disembarking passengers, at the most crowded door for each train at a station where a semi-express train stopped on November 16, 18, and December 6, 2010, was counted from video images. For each station where the train stopped and the stopping stations on the Hanzomon Line, the number of boarding and disembarking passengers was provided every 15 minutes using the metropolitan traffic census for 2005.
(3) Train car dimensions: In order to reconstruct one-quarter of the inside of a Tokyu 5000 Series, the specifications sheet for the train car was used.
(4) Load compensation data: In order to reflect the impact of congestion inside the train on the speed of boarding and disembarking, the number of passengers for the train car with the most crowded door (congestion rate) was acquired. The data are only for the Tokyo 5000 Series that was equipped with a load compensating device 19 weekdays from November 15 to December 10, 2010 from 7:00 to 9:00 am.
(5) Station platform drawings: The width of each station platform was given.

3.3.3 Accuracy of the Model

The reproducibility of the boarding speed, organized by congestion rate in the vehicle, is shown in Figure 6. The horizontal axis shows the door passage speed for individual passengers for each train, in estimated and actual values. It is possible to recreate a situation in which the boarding speed lowers when the rate of congestion increases. Furthermore, the traceability of the door passage speed for each train order is thought to be high.

The reproducibility of boarding and disembarking time measurements for various stations, with types of boarding and disembarkation volumes, is shown in Figure 7. The estimated values in the figure show the average values resulting from 100 simulations using a bar graph and the standard deviation. It can be reproduced with high accuracy.

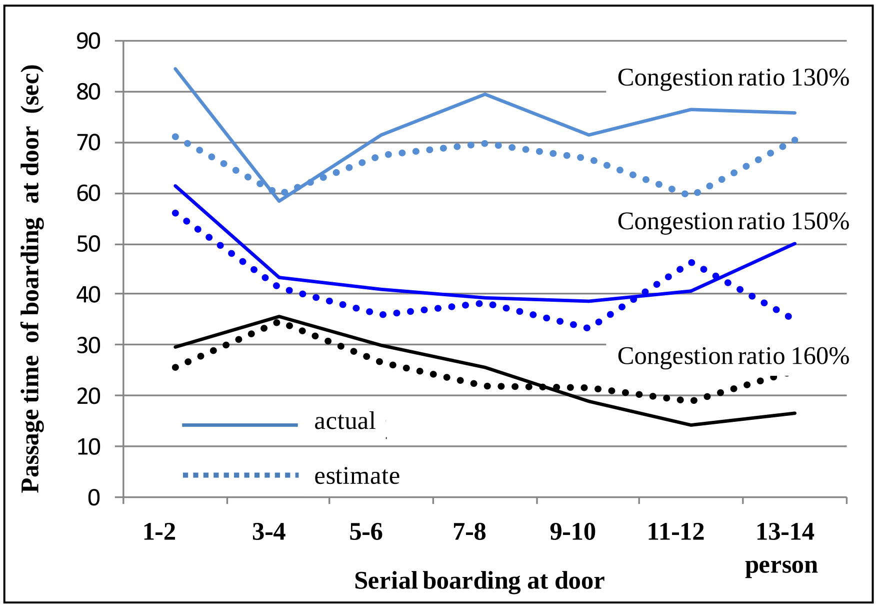

Figure 6. Accuracy of the boarding speed by congestion rate in the vehicle

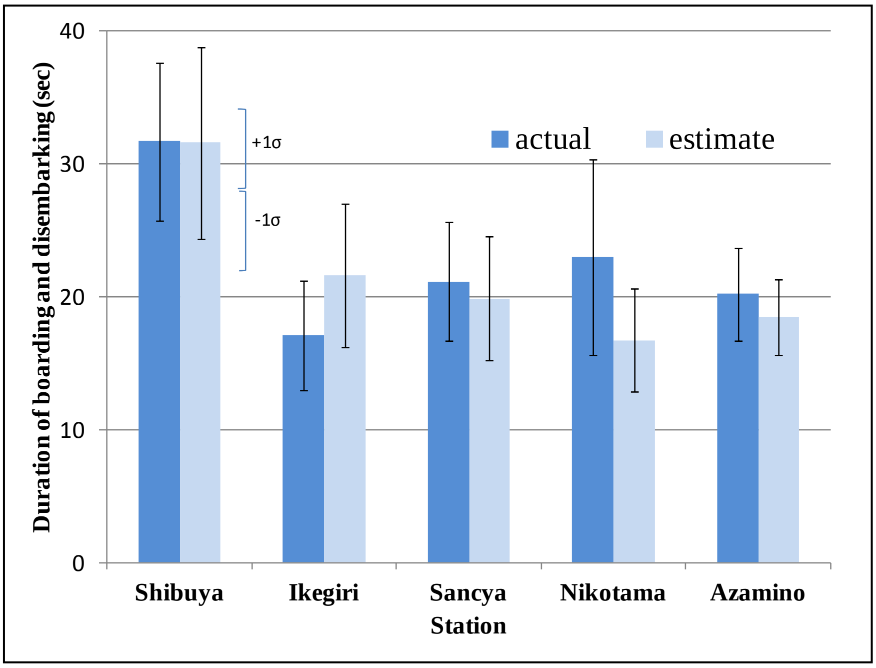

Figure 7. Accuracy of boarding and disembarking time measurements for each stations

3.4 Adjusted Time and Confirmed Time Estimation Model

Rule 1: The adjusted time specifies the time after boarding and disembarking has finished until the time that the doors close. In this model, if boarding and disembarking are completed before the departure time on the time schedule, it is set to leave the doors open until the departure time. In addition, when delayed, the station stopping time is adjusted by adjusting the operation interval, but this cannot be reflected in this model.

Rule 2: The confirmed time specifies the time from the closing of the door until the time of departure, and this is increased because of instances such as getting caught in the door. The confirmed time is thought to be influenced directly and indirectly by the rate of congestion, the number of boarding passengers, and the boarding time, and as a result of three single correlation factors, the rate of congestion was highest with a correlation coefficient of 0.6, so the average value for the confirmed time and the standard deviation, σ, was calculated in 50% rate of congestion units to configure settings that generate these as normal random numbers.

3.5 Model integration

The sub-model above was used to construct an integrated model that simulates knock-on delay. Figure 8 shows some of the simulation screens for the integrated model. Each train is run on the line on the screen to display the boarding and disembarking conditions for each station. For the lines displayed on the screen, the grade of running trains, the block segment length (colored segments in the figure express blocks), the inclination, and the color of the line, change according to the distance between and the train ahead. When a train stops at a station, the disembarking passengers, boarding passengers, continuing passengers, and passenger attributes are displayed, and the color of the station changes depending on whether the train is in the process of being boarded, in the process of confirmation or adjustment, or awaiting departure signals.

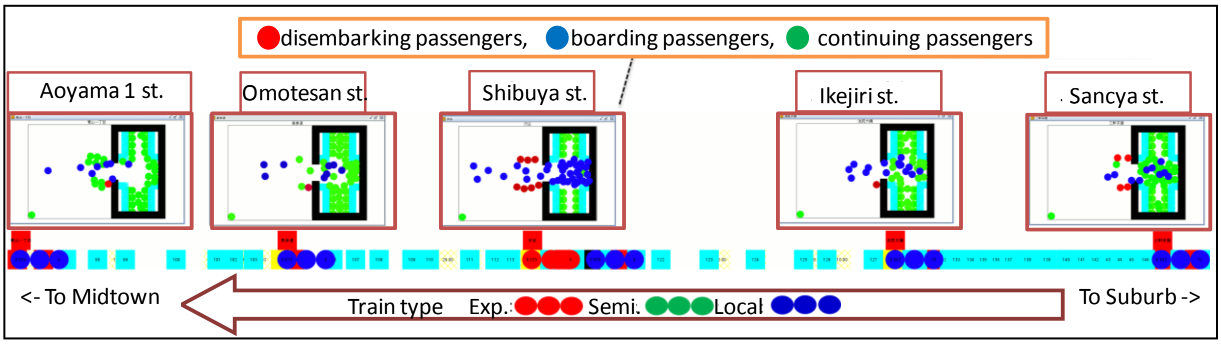

Figure 8. Simulation screens for the integrated model

With the integrated model, the number of boarding passengers changes depending on changes in the train operation interval, so after setting the amount of boarding passengers organized by time on November 25, which had few delays, as the initial value, the number of boarding customers for every train is set to fluctuate moment by movement for each train depending on the condition of delay in the simulation.

Though it is true that the rate of congestion inside the train, or the number of passengers disembarking, changes depending on changes in the number of passengers, because the inclusion of user OD information organized by time is necessary, this cannot yet be reflected in this system.

The Accuracy of the integrated model is shown in Figure 9. Figure 9 shows arrival time delays for Hanzomon Station. The actual value is the average value on November 25 and the estimated value is the average value and standard deviation (±1σ) for ten simulations.

Keeping within the standard deviation on November 25, delays expand towards the peak time and it is understood that behaviors similar to those of actual results are shown. However, the timing in which delays start is early and is an exaggerated estimate until around 9:00, while being underestimated after around 9:30.

In Figure 3, which was explained using the actual delay conditions and factors causing delay on the target lines in Section 2, we explained that it is possible to control the increased stopping time through recovery operation up until the train arriving at Hanzomon Station at 8:00 am, but beyond this it is not possible to absorb the delay through recovery operation, which results in a sudden increase in total delay. As seen in Figure 10, it is understood that the same conditions can be reproduced in this simulation. Furthermore, Figure 11 shows the simulation results demonstrating the knock-on delay conditions at the same station as in Figure 3. Though there is some difference in behavior, it is possible to observe a situation in which delays occurring in the inner-city section propagate to the trains that follow, resulting in the expansion of delays in the inner city as the trains continue in a state where they are unable to absorb delays.

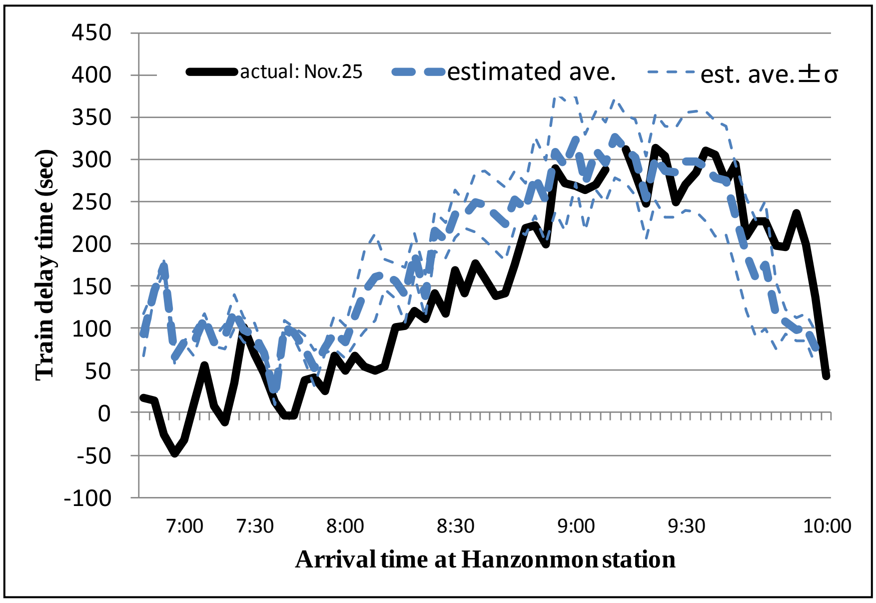

Figure 9. Accuracy of the integrated model

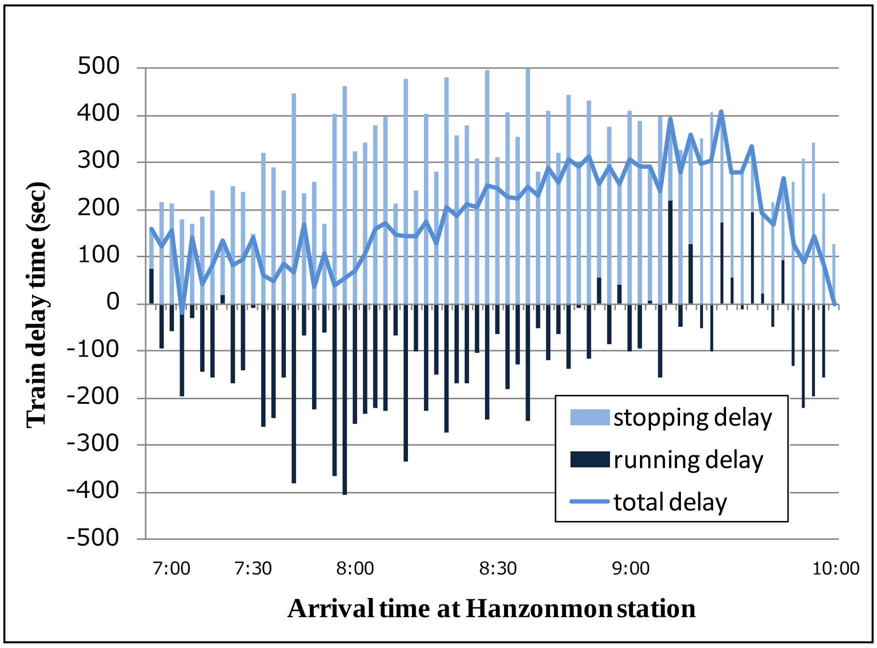

Figure 10. Estimated stopping delays, running delays and total delays for trains arriving at Hanzomon Station

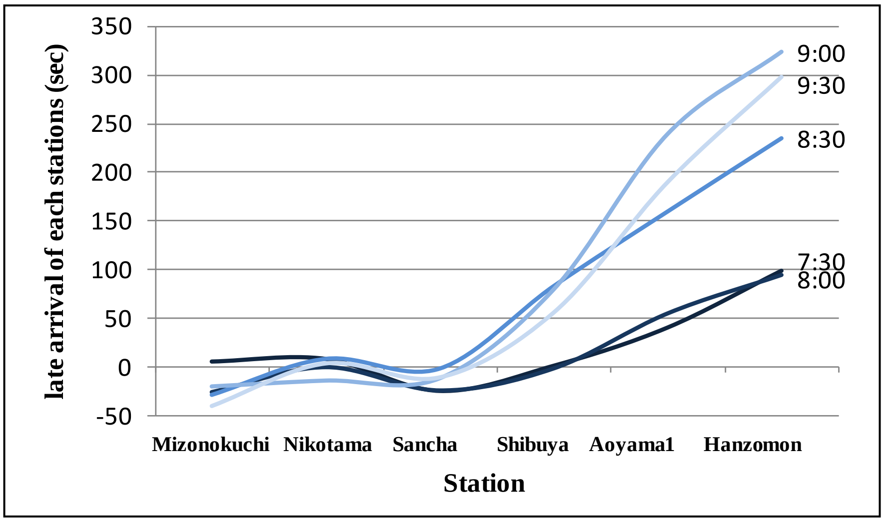

Figure 11. Estimated knock-on train delays for each stations

4. CONCLUSION

The decreasing travel time reliability of urban railway services in the Tokyo Metropolitan Area is the result of the train delays in daily morning hour period.

The goal of this study is to construct a simulation model that is able to quantitatively analyze the effects of anti-delay measures using urban lines that are operated at high frequency on the same track as our target. For the purposes of this study, we have designated a 48.3 km section of tracks running from the Chuo-Rinkan Station on the Tokyu Denentoshi Line to the Oshiage Station on the Tokyo Metro Hanzomon Line as our target.

We developed a simulation model using a multi-agent simulation that includes the running time and stopping time. The errors in the delay estimation of individual trains by the proposed simulator are within the allowable limits in comparison to the actual train delay. Some forecasting results of investment strategies designed to reduce delay can be assessed.

ACKNOWLEDGEMENTS

The authors greatly appreciate the help of TOKYU CORPORATION and Tokyo Metro Co., Ltd. This study was supported by a Grants-Aid Scientific Research (B) 21360242 (Principal researcher: Professor, Dr. Shigeru MORICHI, National Graduate Institute for Policy Studies) from the Japan Society for the Promotion of Science.

REFERENCES

Frank, O. (1966) Two-way traffic in a single line of railway, Operations Research,14, pp.801–811.

Carey, M.,Kwiecinski, A. (1994) Stochastic approximation to the effects of headways on knock-on delays of trains. Transportation Research Part B, 28B (4), 251–267.

Higgins A. and Kozan E. (1998) Modeling train delays in urban networks, Transportation

Science Vol.32, No.4, 346-357.
Huisman T.,Boucherie R.J.(2001) Running times on railway sections with heterogeneous train traffic, Transportation Research Part B 35, 271-292.
Petersen, E.R.,Taylor, A.J. (1982) A structured model for rail line simulation and optimization. Transportation Science, 16, 192–206
Lu Q., Dessouky M.M., Leachman R.C. (2004) Modeling of train movements through complex networks, ACM Transactions on Modeling and Computer Simulation, 14, 48-75.
Li K., Gao Z., Ning B. (2005) Cellular automaton model for railway traffic, J. of Computational Physics 209, 179-192.
Fu Y., Gao Z., Li K. (2008) Modeling Study for Tracking Operation of Subway Trains Based on Cellular Automata, J Transpn Sys Eng & IT, 8(4), 89-95